Chronic Neurotrophin Delivery Promotes Ectopic Neurite Growth From the Spiral Ganglion of Deafened Cochleae Without Compromising the Spatial Selectivity of Cochlear Implants

Thomas G. Landry,[1,2] James B. Fallon,[1,2,3] Andrew K. Wise,[1,2,3] and Robert K. Shepherd[1,2,3]*

[1]The Bionics Institute, East Melbourne, Victoria, 3002, Australia
[2]Department of Otolaryngology, University of Melbourne, East Melbourne, Victoria, 3002, Australia
[3]Department of Medical Bionics, University of Melbourne, East Melbourne, Victoria, 3002, Australia

ABSTRACT

Cochlear implants restore hearing cues in the severe–profoundly deaf by electrically stimulating spiral ganglion neurons (SGNs). However, SGNs degenerate following loss of cochlear hair cells, due at least in part to a reduction in the endogenous neurotrophin (NT) supply, normally provided by hair cells and supporting cells of the organ of Corti. Delivering exogenous NTs to the cochlea can rescue SGNs from degeneration and can also promote the ectopic growth of SGN neurites. This resprouting may disrupt the cochleotopic organization upon which cochlear implants rely to impart pitch cues. Using retrograde labeling and confocal imaging of SGNs, we determined the extent of neurite growth following 28 days of exogenous NT treatment in deafened guinea pigs with and without chronic electrical stimulation (ES). On completion of this treatment, we measured the spread of neural activation to intracochlear ES by recording neural responses across the cochleotopically organized inferior colliculus using multichannel recording techniques. Although NT treatment significantly increased both the length and the lateral extent of growth of neurites along the cochlea compared with deafened controls, these anatomical changes did not affect the spread of neural activation when examined immediately after 28 days of NT treatment. NT treatment did, however, result in lower excitation thresholds compared with deafened controls. These data support the application of NTs for improved clinical outcomes for cochlear implant patients. J. Comp. Neurol. 521:2818–2832, 2013.

INDEXING TERMS: electrical stimulation; auditory nerve; deafness; cochlear implant

In the normal hearing cochlea, hair cells within the organ of Corti induce action potentials in the primary afferent neurons of the auditory nerve (spiral ganglion neurons; SGNs) in response to micromechanical acoustic stimulation. In patients with a severe–profound hearing loss, most commonly caused by loss of hair cells, a cochlear implant is the only therapeutic option available, providing auditory cues by electrically stimulating SGNs. However, the loss of hair cells initiates a gradual degeneration of SGNs, which is observed in both animal models of deafness (Spoendlin, 1984; Leake and Hradek, 1988; Hardie and Shepherd, 1999; Dodson and Mohuiddin, 2000) and in human cochleae (Nadol et al., 1989; Zimmermann et al., 1995; Nadol, 1997; Miura et al., 2002). This SGN degeneration is due, at least in part, to the loss of the endogenous source of the neurotrophin (NT) peptides brain-derived neurotrophic factor (BDNF) and neurotrophin-3 (NT-3), resulting in apoptotic cell death (Alam et al., 2007). These NTs are normally expressed by hair cells (Ylikoski et al., 1993; Ernfors et al., 1995; Tan and Shepherd, 2006; Sugawara et al., 2007) and support cells

Grant sponsor: National Institute on Deafness and Other Communication Disorders, National Institutes of Health; Grant number: HHS-N-263-2007-00053-C; Grant sponsor: The Bartholomew Reardon PhD Scholarship (The Bionics Institute; to TGL); Grant sponsor: The Mabel Kent Scholarship (to TGL); Grant sponsor: Victorian Government's Operational Infrastructure Support Program (to the Bionics Institute).

*Correspondence to: Robert K. Shepherd, The Bionics Institute, 384–388 Albert St, East Melbourne 3002, Victoria, Australia. E-mail: rshepherd@bionicsinstitute.org

Received July 25, 2012; Accepted for publication February 5, 2013.
DOI 10.1002/cne.23318
Published online February 22, 2013 in Wiley Online Library (wileyonlinelibrary.com)

(Stankovic et al., 2004; Zilberstein et al., 2012) of the organ of Corti. Administering exogenous NTs to deafened cochleae rescues SGNs from these degenerative changes (Miller et al., 1997; Shinohara et al., 2002; Gillespie et al., 2003; Richardson et al., 2005; Shepherd et al., 2005; Agterberg et al., 2008; Glueckert et al., 2008; Wise et al., 2011). Associated with this rescue effect is a proliferation in the number of peripheral SGN neurites compared with deafened controls (Wise et al., 2005; Leake et al., 2011). Moreover, in contrast to the highly radial neurite projections observed in normal cochleae, SGNs treated with exogenous NTs often exhibit ectopic neurite growth (Staecker et al., 1996; Wise et al., 2005; Glueckert et al., 2008; Leake et al., 2011).

In the normal cochlea, SGN neurites innervating inner hair cells (IHCs) are spatially arranged along the cochlea in a precise radial path as they project from their soma (Spoendlin, 1969; Liberman, 1982; Bohne and Harding, 1992). The frequency-specific activation of hair cells to acoustic stimulation at spatially restricted cochlear locations leads to activation of localized SGN populations, resulting in a precise tonotopic map. Cochlear implants take advantage of this spatial organization by stimulating different cochlear locations to produce different pitch percepts based on electrode position (Tong et al., 1982; Shannon, 1983). Disruption to SGNs and their neurites as a result of disease and/or therapeutic treatment may result in an increase in the extent of spatial activation of SGNs to intracochlear electrical stimulation (ES), reducing electrode pitch discriminability in implant recipients and leading to reduced speech perception (Henry et al., 2000). Therefore, while producing a number of potentially beneficial effects, such as reduced thresholds to ES (Shinohara et al., 2002; Shepherd et al., 2005; Leake et al., 2011), exogenous NT treatment may have the unintended consequence of degrading speech perception in implant patients by inducing disorganized SGN neurite growth.

We measured the extent of the ectopic growth of SGN neurites and the spread of neural activation to intracochlear electrical stimulation in deafened guinea pigs following chronic NT and/or ES treatment. We have previously reported a significant rescue effect of SGNs in the same NT-treated cochleae, associated with a significant reduction in the auditory brainstem response threshold to ES (Landry et al., 2011). In the present study we report that chronic NT delivery also evokes a significant increase in the extent of neurite growth at the cochlear periphery. Importantly, these changes did not result in an increase in the spread of excitation to intracochlear ES.

TABLE 1.
Experimental Cohorts and Group Numbers[a]

	Unstimulated (US)	Chronically stimulated (ES)
Artificial perilymph (AP)	US/AP, $n = 6$	ES/AP, $n = 4$
BDNF and NT-3 (NT)	US/NT, $n = 5$	ES/NT, $n = 6$
Normal hearing	$n = 5$	

[a]Note that normal hearing animals received no chronic treatment but were deafened during the acute electrophysiological experiment. BDNF, brain-derived neurotrophic factor; NT-3, neurotrophin-3.

MATERIALS AND METHODS

Experimental animals

Twenty-six ($N = 26$) young adult pigmented guinea pigs (300–600 g) of either sex were used. Table 1 summarizes the five cohorts in the study. The treatment procedures are described in detail elsewhere (Landry et al., 2011). Prior to experimental use, all animals were otoscopically normal and had normal hearing thresholds as measured by auditory brainstem responses (ABRs) to acoustic clicks (Landry et al., 2011). All procedures were approved by the Royal Victorian Eye and Ear Hospital Animal Research Ethics Committee.

Deafening, cochlear implantation, and chronic stimulation

Guinea pigs were ototoxically deafened by an intravenous injection of frusemide (130 mg/kg; Troy, Glendenning, NSW, Australia), followed by a subcutaneous injection of kanamycin sulfate (420 mg/kg; Sigma-Aldrich, St. Louis, MO) within 2 minutes of frusemide administration (Shepherd et al., 2005). Animal weight and behavior were closely monitored for the week following aminoglycoside treatment. After 2 weeks of recovery, each animal was anesthetized with ketamine (60 mg/kg; Parnell, Sydney, Australia) and xylazine (4 mg/kg, intramuscular; Ilium), and severe hearing loss was confirmed by an increase of $>$50 dB in ABR thresholds to acoustic clicks. The degeneration of the organ of Corti was also observed histologically following sacrifice (Landry et al., 2011). Under aseptic conditions, the left cochlea was surgically exposed, the round window was opened, and an electrode array was inserted 6 mm into the lower basal turn scala tympani (ST) (Fig. 1A,B). The design of the implant was a modified version of Shepherd and Xu (2002). Briefly, each electrode array included six platinum ring electrodes (0.2 mm wide; 0.4-mm diameter; 0.3-mm interelectrode spacing). Electrodes were numbered from E1 at the apical end to E6 at the basal end. All implants contained a drug delivery

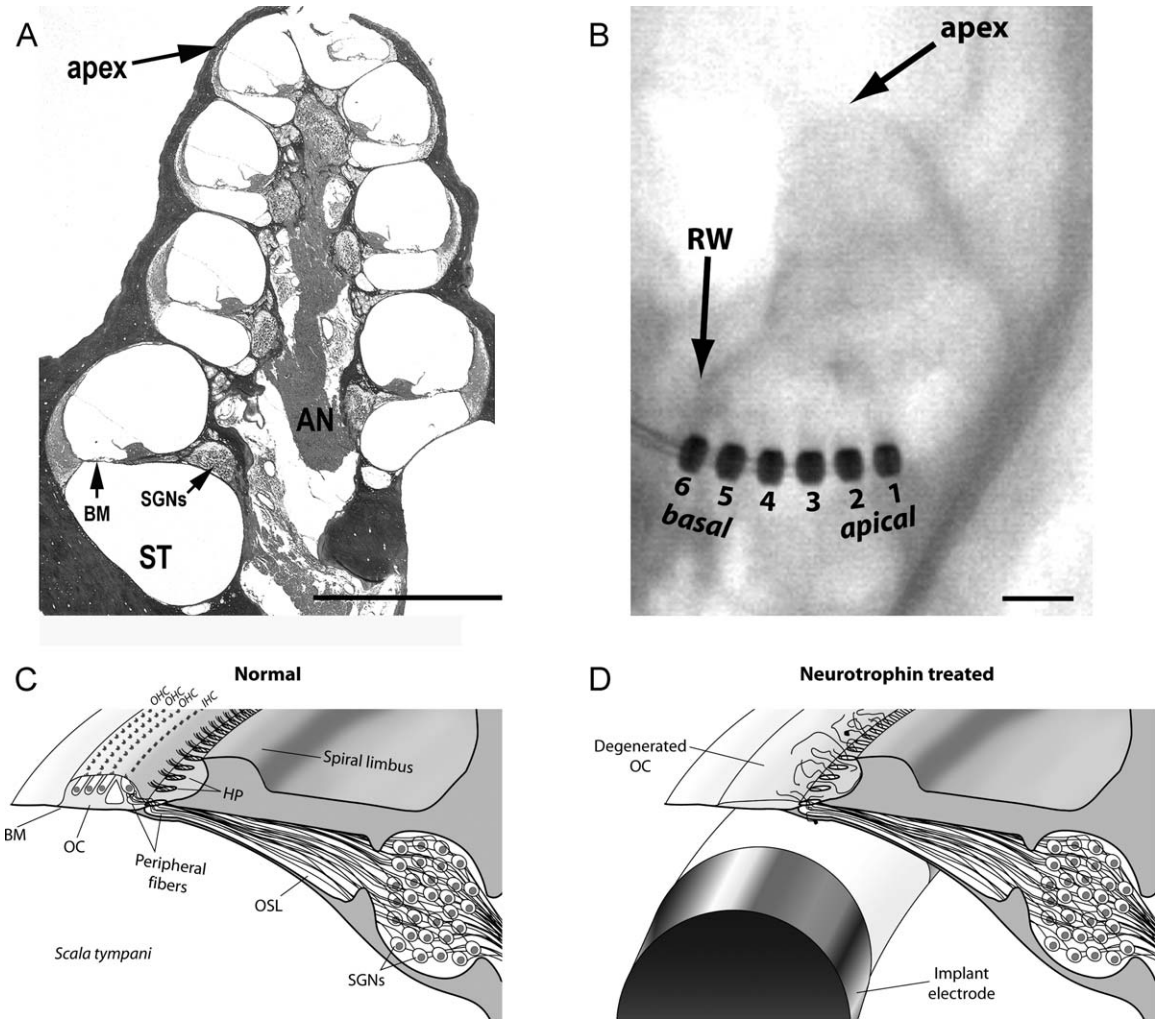

Figure 1. **A:** Low-power photomicrograph of a midmodiolar transverse section through a guinea pig cochlea. This fluid-filled spiral structure has four turns spiraling from the cochlear base to the apex. The scala tympani (ST) is the site of implantation of the intracochlear electrode array. In normal hearing cochlea, the sensory hair cells are located within the organ of Corti on the basilar membrane (BM). The cell bodies of the spiral ganglion neurons (SGNs) reside in a small cavity adjacent to the ST. These bipolar neurons have a peripheral neurite that projects to the hair cells on the BM and a central axon that projects to the brainstem via the auditory nerve (AN). **B:** An x-ray of a guinea pig cochlea with an electrode implanted into the ST via the round window (RW). The electrode array contained six platinum rings (numbered) and a drug delivery cannula used to release neurotrophins or artificial perilymph just apical to electrode 1. **C:** Schematic diagram of the sensory epithelium and SGNs of the normal guinea pig cochlea illustrating the highly radial projection of the peripheral neurites from their SGN soma to the sensory hair cells located within the organ of Corti (OC). The peripheral neurites pass through the habenula perforata (HP), small openings in the bony osseous spiral lamina (OSL), where the majority of neurites form a synapse with the closest inner hair cell (IHC). For clarity, the tectorial membrane and Reissner's membrane are not illustrated in this diagram. **D:** Schematic diagram of a deafened cochlea showing a section of an electrode array within the ST and loss of hair cells and OC following deafness. Normally, cochleae such as this would exhibit a significant reduction in the number of peripheral fibers and a loss of SGNs. However, in this example the cochlea has been treated with neurotrophins, rescuing the SGNs from degeneration and producing ectopic growth of neurites beyond the HP. OHC, outer hair cells. Scale bar = 1 mm in A,B.

cannula that was attached to an osmotic pump (200 μl capacity; 28-day delivery period; 0.25 μl/hr; Alzet, Cupertino, CA) containing artificial perilymph (AP) or NTs (30 μg/ml each of BDNF and NT-3; human recombinant; PeproTech, Rocky Hill, NJ) dissolved in AP. Osmotic pumps were surgically positioned subcutaneously between the scapulae. The electrode array lead was fixed to the temporal bone with dental cement and exited the skin via a percutaneous connector (Shepherd et al., 2005). Electrically evoked ABR thresholds were then determined for ES across all bipolar electrode combinations (bipolar electrode separations are given as BP+x, where x is the number of inactive electrode rings between the anode and cathode).

Five days after implantation, the ES cohorts commenced their chronic stimulation program by connecting the percutaneous connector to commercial cochlear implant stimulus generation hardware (CI22 stimulator and ESPrit 3G speech processor; Cochlear, Macquarie University, NSW, Australia) placed in a backpack worn by the animal (Fallon et al., 2009). Chronic ES was delivered sequentially to three bipolar pairs (E1–2, E3–4, and E5–6). Stimuli consisted of charge-balanced biphasic current pulses (100-μs phase duration, 50-μs interphase gap) presented at 1,200 pulses per second (pps) per channel (total rate 3,600 pps) continuously over a 28-day treatment period. Stimulus intensity was programmed to be in the range −3 to +6 dB (re: electrically evoked ABR threshold) per channel (Fallon et al., 2009). An additional two cohorts received NT or AP without receiving ES (unstimulated [US] cohorts in Table 1).

Recording from the inferior colliculus

Following the 28-day treatment period, an acute terminal experiment was performed to record multiunit neural activity in the inferior colliculus (IC) to intracochlear ES (Snyder et al., 2004) and to apply a retrograde neural tracer to the trunk of the auditory nerve (AN) in order to trace individual SGN neurites.

Guinea pigs were anesthetized as described above, and body temperature was maintained at 37°C with a heat pad. The head was placed in a stereotaxic frame, and the IC contralateral to the implanted cochlea was exposed. Neural activity was recorded by using a 32-channel single-shank silicon substrate electrode array (NeuroNexus, Ann, Arbor, MI) with electrode spacing of 100 μm center to center and impedances of 1–1.5 MΩ. The array was mounted on a micromanipulator (2662 Micropositioner; Kopf, Tujunga, CA) and advanced across the cochleotopic axis of the central nucleus of the IC (ICC) at 45° from the midline (Martin et al., 1988). Fluorescent dye was deposited on the recording array in order to verify its location within the ICC histologically (Lim and Anderson, 2007).

Single and multiunit activity was recorded simultaneously from the 32 channels in response to intracochlear ES by using a Cerebus recording system (Blackrock Microsystems, Salt Lake City, UT) at a sampling frequency of 30 kHz per channel. The signal was digitally band-pass-filtered (0.25–7.50 kHz), and the spike detection threshold was set at a voltage between −3.75 and −4.0 times the root mean square of the noise floor for each channel in order to detect spike activity above the noise floor. Input/output functions were determined across all IC recording sites for each stimulating electrode pair by using bipolar ES (parameters identical to the chronic ES program). Stimuli were delivered in a randomized fashion over a range of 0–2 mA in 25-μA steps (or to 50 μA below the threshold for stimulus-induced muscle activation) at a rate of 5 pps for 20 repetitions.

In normal hearing controls, the head was secured with hollow ear bars to allow for closed-field acoustic stimulation. The IC was exposed, and a recording array inserted as described above. Using in-house designed software, pure tone bursts (50-ms duration; 1-ms linear rise/fall) were generated with randomly varying frequency (0.625–10 kHz at 2/octave, and 10–40 kHz at 4/octave) and intensity (0–80 dB SPL, in 5-dB steps) for 20 repetitions. Acoustic stimuli were delivered via a Tucker Davis Technologies (Tulsa, OK) Series II D/A converter (200-kHz sampling) and Vifa XT25TG-30-04 tweeter speaker (Speakerbits, Port Melbourne, VIC, Australia). Following multichannel recording of IC responses to acoustic stimulation, the left cochlea was surgically exposed and acutely deafened by perfusing the ST with 10% neomycin sulfate in order to prevent electrical activation of hair cells (Black et al., 1983). A cochlear electrode array was then acutely implanted, and IC responses to ES were recorded.

Auditory nerve tracing

Following the completion of IC recordings, the left AN trunk exiting the internal auditory meatus was exposed by using a dorsoventral approach (Evans, 1972). A quartz glass micropipette (P-2000 model pipette puller; Sutter Instrument, Novato, CA) with a tip diameter of 20–25 μm was front-filled with 5 μl of 15% biotinylated dextran amine (BDA; 3 kD; lysine-fixable; Invitrogen, Carlsbad, CA) in 0.1 M sodium–citrate–HCl (pH 3.0) (Reiner et al., 2000). The micropipette was advanced through the AN at a rate of 10 μm/s by using a micromanipulator, and the tracer was pressure injected by using a PV830 pneumatic pump (World Precision Instruments, New Haven, CT) at 20 psi in 10-ms pulses (∼20 nl per pulse) at 2 pps. The pipette was advanced 1.5 mm, the injection was stopped, and the pipette was left in place for 10 minutes before being withdrawn. The exposure was flushed with saline, and then the injection protocol was repeated at a second AN location.

After allowing 3 hours for the tracer to diffuse within the SGNs, each animal was overdosed with sodium pentobarbital (150 mg/kg; i.p.) and transcardially perfused with 0.9% NaCl (37°C) followed by 4% paraformaldehyde in 0.1 M phosphate-buffered saline (4°C, pH 7.35). The cochleae were isolated, postfixed overnight in 4% paraformaldehyde (4°C), and then placed in ethylenediamine tetraacetic acid in phosphate-buffered

saline at room temperature for a period of 2 weeks to complete decalcification. The midbrain was isolated and sectioned at 80 μm in the coronal plane by using a vibrating microtome, and stained with thionin for verification of recording array placement within the ICC.

Cochlear histology

The lower basal turn of each cochlea adjacent to the electrode array was prepared for histological examination by using surface preparation techniques and immunolabeled for neurofilament (NF200; 200 kD) as a tissue marker for SGNs and their peripheral neurites (Wise et al., 2005, 2011). Briefly, tissue was incubated in 2% goat serum, followed by anti-NF200 polyclonal rabbit antibodies (1:400; Sigma-Aldrich, N4142) for 48 hours, and finally with anti-rabbit goat antibodies (1:200; Alexa 488-conjugated; Sigma-Aldrich) and NeutrAvidin (0.033 mg/ml; tetramethylrhodamine conjugated; Invitrogen) for 2 hours to label NF200 and BDA, respectively. The preparations were then mounted on slides with 100% glycerol.

Data analysis: surface preparations

Lower basal turn surface preparations were imaged with an LSM 510 confocal microscope (Zeiss, Oberkochen, Germany). SGN neurites were traced and the position of the habenula perforata (HP; Fig. 1C) recorded in LSM Image Browser software (Zeiss). HPs were visible as dark regions in the background fluorescence from which the neurite emerged onto the basilar membrane. NF200 labeling was used to trace neurites, although single traceable neurites were more reliably observed with BDA labeling.

Several measurements were made from the traced neurites to quantify the extent of ectopic growth (Fig. 2). First, the degree of lateral deviation of each neurite was determined by measuring the sum of its greatest deviation in both the basal and apical directions relative to a radial axis. Second, the length of the neurite was measured from the HP. Finally, to determine whether ES or NT treatments provided significant guidance cues, the distance from the HP to the tip of the neurite was divided by its total length ("directionality"; Fig. 2), with lower values indicating an increased ectopic growth pattern.

Data analysis: inferior colliculus recordings

Recorded IC data were analyzed by using customized data analysis packages in Igor Pro 6.10 software (WaveMetrics, Lake Oswego, OR). A 3–33-ms poststimulus spike detection window was used. The number of spikes detected was averaged across trials for each stimulus condition at each recording location. Each datum was normalized between the spontaneous activity rate and maximum response for any stimulating electrode according to the formula:

$$RN_i = (R_i - S_i)/(M_i - S_i)$$

where RN_i is the normalized value for a given stimulus at the ith recording electrode, R_i is the average spike count, S_i is the spontaneous firing rate (average rate in a 33–3-ms prestimulus window prior to all stimuli), and M_i is the maximum firing rate recorded at each recording location for any stimulus. The data were also smoothed across the matrix with a 3×3 Gaussian function (normalization and smoothing functions from Snyder et al., 2008).

Threshold (defined as a response 30% above the spontaneous activity) was determined for each of the 32 recording sites across the IC (see Fig. 4B for a 10-kHz acoustic stimulus). This definition of threshold is consistent with previously published work (Snyder et al., 2008). Thresholds at 30% above spontaneous activity follow the boundary of the response images and capture the broader activation seen with more widely spaced bipolar pairs. Although a lower percentage or a threshold measure based on d′ might give a wider extent of activation, this would be true across all conditions, and therefore would be unlikely to affect the group comparisons. Mean first spike latency and jitter (standard error of the mean [SEM] of latency) were also examined across recording sites. Response intensity data are displayed across the IC as "spatial response images"—juxtaposed input/output data for each of the 32 IC recording sites—revealing the spread of activation across the IC for either acoustic or electrical stimuli (Fig. 4D,F). Finally, to determine the spread of neural activation across the IC, a spatial tuning curve (STC) was produced at threshold for each ES electrode, and the STC widths were measured at 1–6 dB above threshold as a measure of the spread of activation across stimulus amplitudes.

RESULTS

Analysis of neurite growth

All labeled SGN neurites in the region of the cochlea adjacent to the electrode array were examined. The BDA-avidin labeling method used labeled only a small proportion of neurites in the majority of cochleae, allowing unambiguous tracing of single neurites. The number of traced neurites used for statistical comparisons for each cohort was: normal control $n = 50$, US/AP $n = 65$, US/NT $n = 19$, ES/AP $n = 23$, ES/NT $n = 42$, consisting of 155 tracer labeled and 44 NF200-labeled fibers.

Representative examples of tracings are shown for each cohort in Figure 2. Neurites from the normal

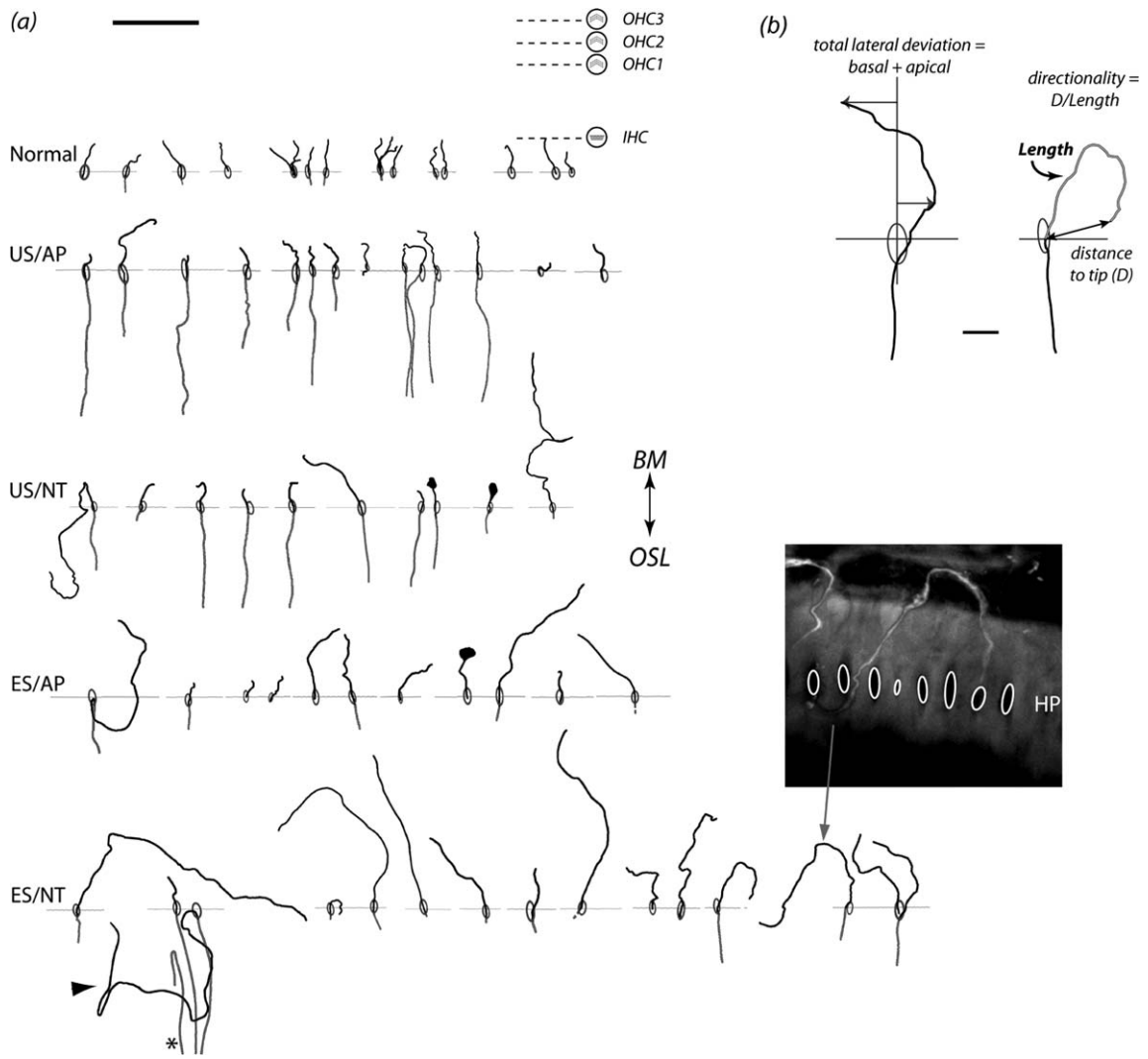

Figure 2. **A:** Representative examples of SGN neurite tracings for each treatment group. Ovals indicate habenula perforata (HP), and horizontal lines indicate the local HP plane for each neurite (aligned for all traces). For reference, the approximate locations of the inner (IHC) and outer hair cells (OHC) are shown associated with the normal cochleae. Nearly all neurites traced in the normal group terminated near the IHCs. These tracings illustrate neurites outside the osseous spiral lamina (OSL). Across all treatment groups the majority of neurites projected toward the basilar membrane (BM), although some projected in the opposite direction toward the spiral limbus (e.g., arrowhead). A small number of neurites performed a hairpin turn within the OSL prior to emerging from the HP (e.g., asterisk). Note the swelling at the tip of some neurites. The inset shows a confocal image of a BDA-labeled neurite (arrow indicates the corresponding tracing). **B:** Example traces showing the derivation of pathway quantification measures of lateral deviation, total neurite length, and directionality. See Table 1 for treatment groups. Scale bar = 50 μm in A; 10 μm in B.

animals were typically short (~10 μm from the HP) and radial, and terminated at the level of the closest IHC. In contrast, neurites across all deafened treatment groups exhibited greater variability in length and an increase in deviation from a radial projection compared with the normal controls. Cochleae treated with ES/NT showed the most ectopic growth patterns. In the few instances in which labeled neurites were able to be visualized within the osseous spiral lamina (OSL), their projection profiles were typically similar to that observed in normal cochleae, although evidence of an ectopic projection was occasionally observed (Fig. 2A).

The group data illustrating neurite lateral deviation, length, and directionality are shown in Figure 3A–C, respectively. The length and lateral deviation data were not normally distributed; therefore statistical comparisons were performed by using rank transformations of these data (normal cohort excluded from ranking). In two-way analyses of variance (ANOVAs; AP–NT, US–ES factors), NT-treated animals showed a significant

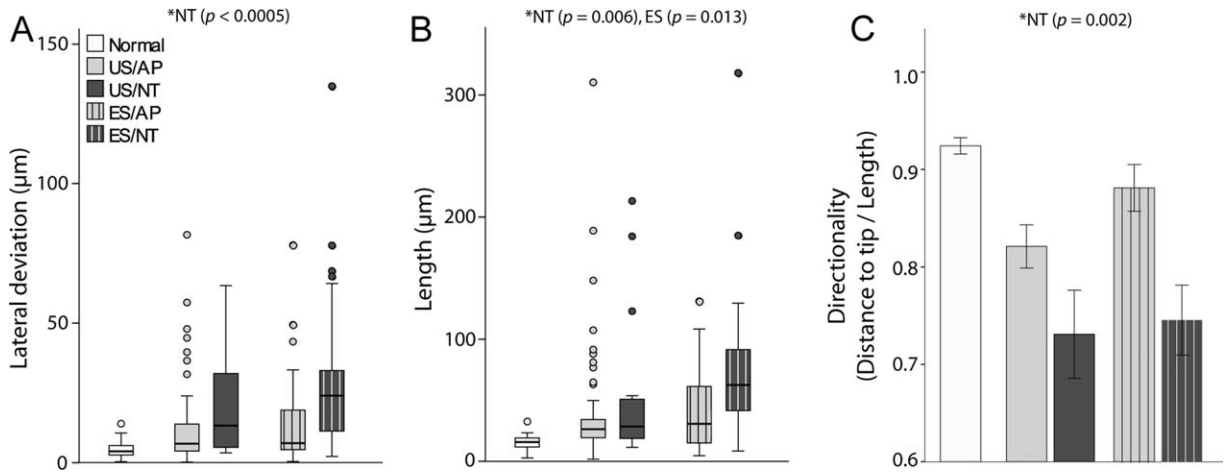

Figure 3. Group data for (**A**) neurite lateral deviation, (**B**) length, and (**C**) directionality. Significant differences were observed in the NT versus AP cochleae for each measure (*, two-way ANOVA; performed on ranks for lateral deviation and length), as well as significantly greater neurite length in ES animals. The data for normal animals are shown for comparison but were not included in the statistics. US, unstimulated; ES, electrically stimulated; AP, artificial perilymph; NT, neurotrophin treatment. Lateral deviation and Length show median, quartiles (box) and 1.5 times beyond the interquartile range (bars). Directionality error bars ± 1 SEM. See Table 1 for treatment groups.

increase in neurite length (F [df_{error} 145] = 7.654, $P = 0.006$) and lateral deviation ($F = 13.943$, $P < 0.0005$), and a decrease in directionality ($F = 11.278$, $P = 0.001$) compared with animals treated with AP. Significantly greater neurite length was also seen in ES animals compared with US ($F = 6.385$, $P = 0.013$). All other main effects and interactions were not statistically significant ($P > 0.05$). Directionality of neurites appeared to be quite high in ES/AP compared with other treatment groups despite no significant interactions, but an *a posteriori* independent samples *t*-test between US/AP and ES/AP directionality rank means confirmed no significant difference ($P > 0.05$). To determine the effects of long-term deafening and cochlear implantation without ES or NT treatment, independent samples *t*-tests were performed between US/AP and normal controls, with significant differences for neurite length ($t = -7.060$), lateral deviation ($t = -4.359$), and directionality (t [df 113] = 3.909; $P < 0.0005$ for each measure).

The majority (83%) of neurites projected from the HP toward the basilar membrane, whereas a small proportion projected in the opposite direction (i.e., towards the spiral limbus; Fig. 2). Neurites were also occasionally observed within the ST; most contained a bulbous structure at the tip of the neurite.

Inferior colliculus recordings

Neural responses to ES were recorded across the cochleotopically organized ICC to examine the effects of ectopic neurite growth on the spread of SGN activation. Histological examination of the IC verified that the recording array was optimally located in the ICC in all but one animal (data not shown). Data from this normal control animal were excluded, giving the following animal numbers per cohort: normal $n = 4$, US/AP $n = 6$, US/NT $n = 5$, ES/AP $n = 4$, and ES/NT $n = 6$.

Basic response properties

Figure 4A illustrates typical multiunit activity after acoustic stimulation recorded at individual recording sites across the ICC in a normal hearing animal. Two IC regions with low thresholds to a given frequency were seen (Fig. 4D), corresponding to the ICC and the external nucleus of the IC (ICX). Fine frequency tuning, characteristic of the ICC, is evident within individual ICC locations (Fig. 4B), whereas fine spatial tuning to pure tones can be seen across the ICC (Fig. 4D). The characteristic frequency (CF) varied systematically across the ICC, with lower CFs dorsolaterally and higher CFs ventromedially (Fig. 4C).

Electrically evoked ICC activity exhibited mean first spike latencies in the range 3.6–6.0 ms. Response thresholds (0.30 normalized response intensity) were examined for BP+0 (adjacent bipolar) stimulating electrodes for the "best recording location" (i.e., the ICC location with the lowest threshold). A repeated measures ANOVA showed no significant effect of BP+0 configuration on threshold across all animals ($P > 0.05$), indicating that E1–2, E2–3, E3–4, and E4–5 yielded similar thresholds within animals (data for the bipolar

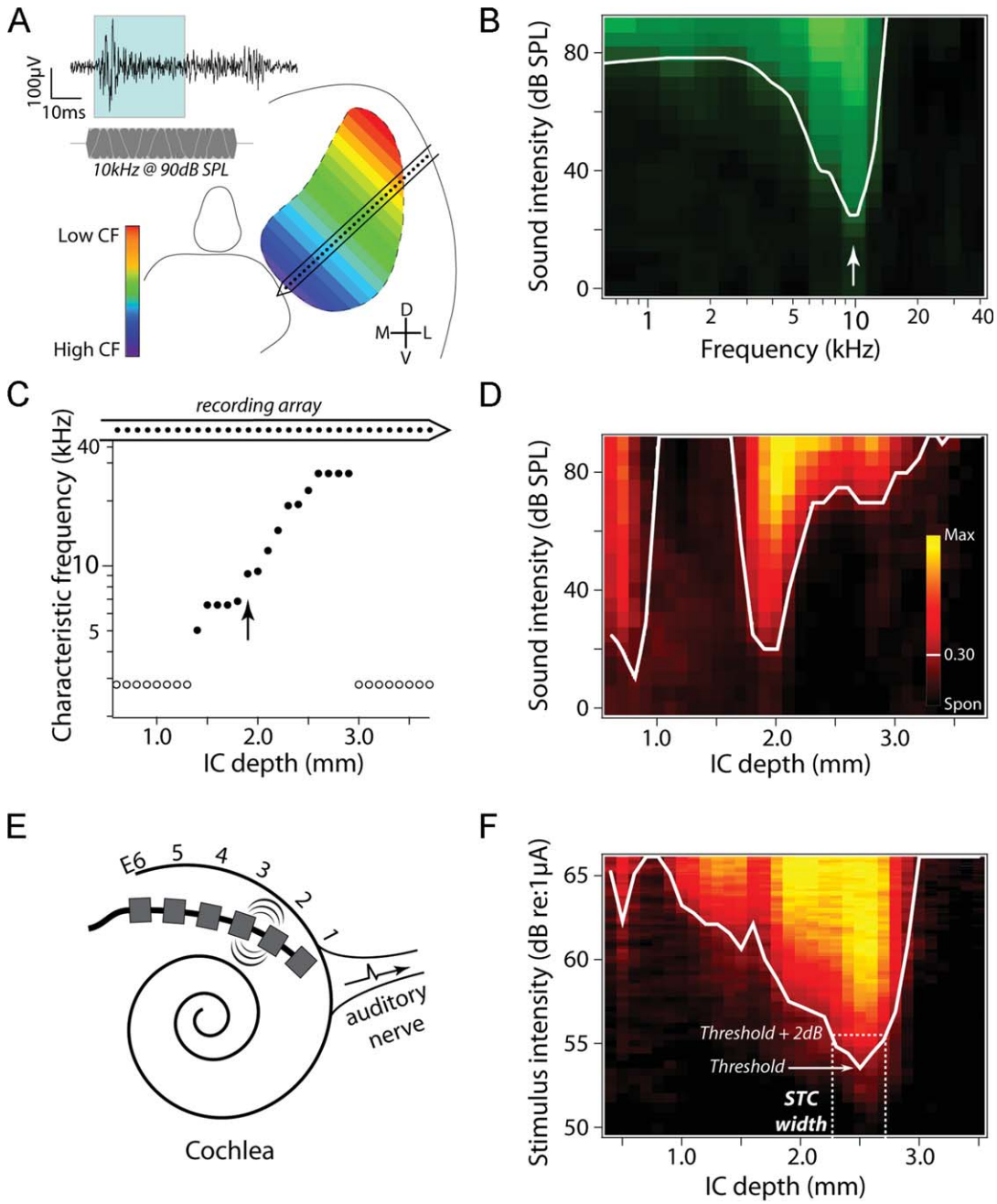

Figure 4. Overview of multichannel inferior colliculus (IC) recording techniques in both normal hearing (to pure tones) and deafened animals (to electrical stimulation via a stimulating electrode array in the cochlea). **A:** Multichannel recordings along the cochleotopic axis of the central nucleus of the inferior colliculus (ICC). The inset shows a representative recording from a single ICC recording site on the 32-channel electrode array (indicated by dots on the recording array in A and C) showing the response to a 10-kHz tone burst (shown below the recording trace). The shaded region shows the 3–33-ms poststimulus spike counting window used in this study. **B:** The frequency tuning curve at the recording site indicated by the arrow in C (black = 0 spikes, light green = 12 spikes, white line = 0.30 response intensity, arrow = characteristic frequency). **C:** The characteristic frequency (CF) as a function of recording site within the ICC of a normal hearing animal illustrating the cochleotopic organization of the ICC. Open circles indicate ICC locations where CF could not be reliably determined. **D:** IC spatial response image to a 10-kHz tone burst illustrates neural activity recorded across the spatial extent of the IC to a fixed stimulus while intensity is varied across the dynamic range (black = spontaneous firing rate, yellow = maximum rate). These data are used to construct spatial tuning curves (STC; white lines = 0.30 response intensity) that illustrate the spatial extent of neural excitation across the IC. **E:** Schematic diagram of the six-ring stimulating electrode array implanted into the deafened cochlea. Stimulation of specific electrode pairs excite different subpopulations of SGNs across the cochleotopic gradient (e.g., E2–3). This cochleotopic output of the SGNs forms the basis of cochleotopic excitation patterns in the auditory pathway, including in the ICC. **F:** Representative spatial response image and STC to stimulation of bipolar electrodes E4–5 in an US/AP animal. Note that the spatial extent of excitation via bipolar electrical stimulation is much greater than that evoked acoustically in normal hearing animals (compare with D). The derivation of STC width at 2 dB above threshold is illustrated here by the dashed lines.

TABLE 2.
Mean Electrically Evoked ICC Thresholds using a BP+0 Stimulating Electrode Configuration for Each Experimental Group

Treatment group	*n*	Mean (μA)	SEM
Normal	4	475.0	96.9
US/AP	6	555.2	66.9
US/NT	5	447.5	89.2
ES/AP	4	1,107.8	111.8
ES/NT	6	657.3	72.8

See Table 1 for treatment groups. ICC, central nucleus of the inferior colliculus.

electrode pair E5–6 were typically excluded, as responses evoked by these electrodes were often contaminated by myogenic activity). The mean best location threshold for BP+0 electrodes was calculated for each animal, and treatment group means were compared with a two-way ANOVA (AP–NT, US–ES factors; normals excluded; Table 2). Significantly higher thresholds were found for ES animals compared with US ($F[df_{error}\ 17] = 20.92$, $P < 0.0005$), and significantly lower thresholds were found in NT animals compared with AP ($F = 11.22$, $P = 0.004$), with no significant interaction ($P > 0.05$).

Spread of activation to electrical stimuli

Similar to IC recordings after acoustic stimuli in normal hearing animals, the spatial response images for ES typically showed two regions of low threshold activation corresponding to the ICC and ICX. This is evident in the spatial response images shown in Figure 5A. The STC minimum in the ICC shifted to the right (i.e., ventromedially) with more basal cochlear stimulation (compare minima evoked by apical electrode pair E1–2 with the basal pair E5–6 in Fig. 5). Within each cohort, increasing the BP electrode separation caused significant decreases in ICC threshold (linear regression ANOVAs, $P < 0.05$; compare ICC minima for narrow bipolar pair E1–2 (BP+0) with the broad bipolar pair E1–6 (BP+4); Fig 5B).

Because BP+0 electrodes produce the most spatially restricted ICC STCs (Fig. 5A), data generated from this stimulating electrode geometry were examined for variation in the spread of activation across treatment groups. The STC width for all groups increased with increasing stimulus intensity, and the rate of increase was similar across the cohorts (Fig. 6). The two ES-treated cohorts (ES/AP and ES/NT) showed greater STC widths compared with US cohorts (US/AP and US/NT) and normal animals. To compare the groups statistically, two-way ANOVAs were performed (US–ES and AP–NT factors) on the mean BP+0 (E1–2, E2–3, E3–4) STC widths at 1, 2, 4, and 6 dB above threshold. To correct for the multiple comparisons, a type I error rate of 0.05 was adjusted to 0.0125 for these tests.

Although we observed a significant increase in BP+0 STC width in ES-treated animals compared with US animals at 1 dB ($F[df_{error}\ 17] = 27.305$, $P < 0.0005$) and 2 dB above threshold ($F = 15.989$, $P = 0.001$), there was no significant effect of NT or treatment interaction at any stimulus level tested. Independent samples *t*-tests between US/AP and normal controls showed no significant difference at 1, 2, 4, or 6 dB above threshold.

Relationship between spread of activation and threshold

ES animals had both significantly higher ICC thresholds and significantly broader STCs than US animals at 1 and 2 dB above threshold. ICC threshold and STC width data were examined together to determine whether there was a significant relationship between the two measures. Figure 7 shows the within-animal mean threshold for E1–2, E2–3, and E3–4 plotted against the mean STC width at 2 dB above threshold for the same cochlear electrodes. Lower electrical thresholds were statistically correlated with narrower STC widths (Pearson's correlation, $r^2 = 0.311$, $P = 0.004$). To investigate whether SGN survival was a factor in this observation, data from normal animals were examined (Fig 7B). Normal controls were chosen because there was much less variability in the SGN density of this cohort compared with the treatment groups (Landry et al., 2011). A significant correlation was evident across BP+0 electrodes within the normal cohort (E1–2, E2–3, E3–4) ($r^2 = 0.482$, $P = 0.018$; Fig 7B), indicating that the correlation seen in deafened cohorts was not dependent on SGN survival.

DISCUSSION

We have demonstrated that exogenous NT delivery in deafened cochleae that results in significant rescue of SGNs and a concomitant reduction in EABR thresholds (Landry et al., 2011) will also promote significant ectopic growth of SGN neurites. Importantly, these anatomical changes do not affect the extent of spatial activation of SGNs to ES, as measured by spatial tuning curves recorded in the auditory midbrain.

Ectopic peripheral neurite growth

Previous studies have examined the morphological response of SGN neurites following noise-induced hearing loss (Bohne and Harding, 1992) or chemical deafening combined with exogenous NT treatment (Wise et al., 2005, 2011; Shibata et al., 2010; Leake et al.,

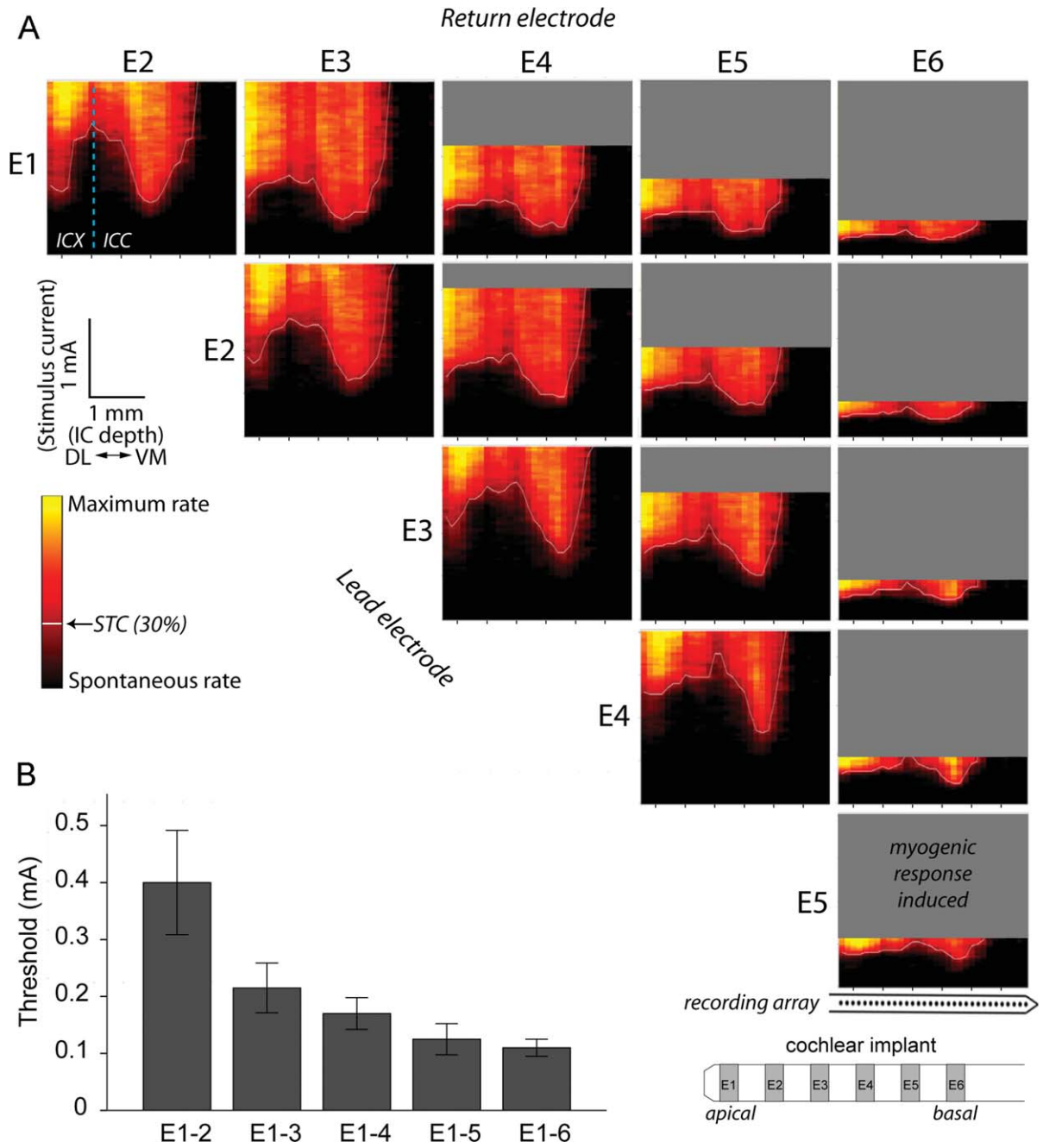

Figure 5. **A:** Representative spatial response images across the cochleotopic axis of the inferior colliculus (IC) for each bipolar stimulating electrode from an unstimulated/neurotrophin-treated animal (US/NT). As the site of stimulation is moved from an apical (E1) to a more basal (E6) stimulation site in the lower basal turn of the cochlea, the minima of spatial tuning curves (STC; white lines) recorded within the central nucleus of the inferior colliculus (ICC) occurred at more ventromedial (VM) locations (to the right in each panel). As the interelectrode distance increased, the IC response threshold decreased, and the myogenic threshold also decreased (gray areas). Responses were usually recorded within the external nucleus (ICX) as well, as seen at the dorsolateral (left) recording locations in this example. The dashed line in the E1–2 response panel indicates the physiological boundary between the ICC and ICX. Response intensities have been smoothed and normalized between spontaneous (black) and maximum rate (yellow). Note that the stimulus amplitude (y-axis) is scaled linearly from 0 to 2 mA in this figure due to the large range of thresholds across stimulating electrode configurations. **B:** Mean ICC thresholds decreased with increasing electrode separation (representative data from the US/NT cohort). Error bars ± 1 SEM.

2011). Some of the projection patterns described in these studies, including neurite projection toward the spiral limbus, were also observed in the present study. However, few studies have quantified neurite growth patterns in both deafened and chronic NT/ES-treated animals (Leake et al., 2011; Wise et al., 2011).

We hypothesized that a significant increase in lateral deviation associated with chronic NT treatment would disrupt the cochleotopic organization of SGNs to ES via a multichannel electrode array located within the scala tympani. However, the extent of the lateral deviation observed following a 1-month treatment with NT was small (typically <100 μm) compared with the dimensions of the typical electrodes used in contemporary cochlear implants (see Fig. 1D, in which ectopic neurite growth and an individual platinum electrode are drawn to scale). Given these large differences in dimensions, it is not surprising that there was no significant relationship between chronic NT treatment and the spread of activation to intracochlear ES. It is important to note, however, that longer periods of chronic NT delivery, or treatment in other species/etiologies, may yield more extensive ectopic projections that could result in altered spatial excitation patterns.

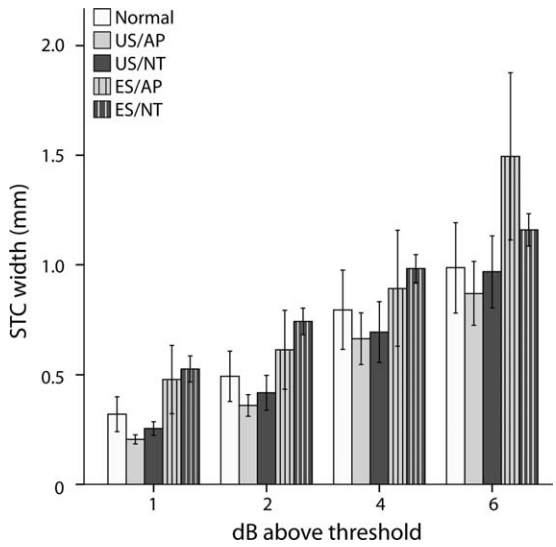

Figure 6. Group means for BP+0 spatial tuning curve (STC) width. A significant increase in width was observed in electrically stimulated (ES) animals at 1 and 2 dB above threshold ($P < 0.0125$; two-way ANOVAs). Means for normals are shown for comparison but were not included in the statistics. Error bars ± 1 SEM. See Table 1 for treatment groups.

We reported similar resprouting of SGN neurites in a previous study of deafened guinea pigs after intracochlear delivery of the same NTs over the same duration (28 days) using a higher NT concentration of 50 μg/ml (vs. 30 μg/ml in the present study) (Wise et al., 2005). Some neurites looped back upon themselves within the osseous spiral lamina whereas others meandered along the basilar membrane and formed a disorganized tangle of processes. Similar ectopic projection patterns were observed in the present study despite lower NT concentrations and different neurite labeling techniques (Fig. 2A).

Whereas ectopic neurite growth in the present study and that of Wise et al. (2005) were associated with high concentrations of exogenous NT delivered via osmotic pumps, neurite growth was also evident in studies using cell-based techniques in which the quantity of NT delivered is expected to be at physiological levels (Shibata et al., 2010; Wise et al., 2010; Wise et al., 2011). In long-term deafened cats, neurites were observed to project into both the cellular epithelial layer on the inner sulcus and the scala tympani (Wise

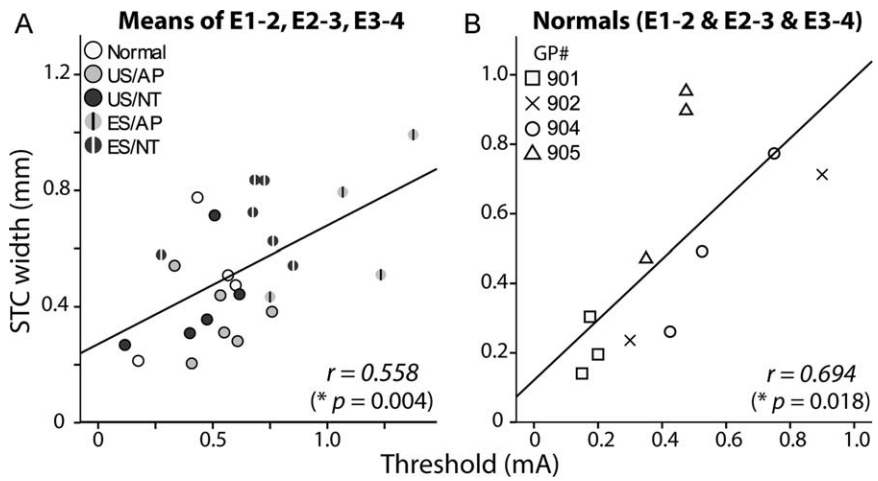

Figure 7. Scatterplots showing central nucleus of the inferior colliculus (ICC) threshold versus spatial tuning curve (STC) width at 2 dB above threshold. **A:** A significant correlation was observed across all animals for the within-animal mean STC width and threshold for BP+0 electrode combinations E1–2, E2–3, and E3–4 (*, two-tailed Pearson's correlation). **B:** A significant correlation was also found across these stimulating electrodes in acutely deafened normal animals. See Table 1 for treatment groups.

et al., 2011). Given the similar response of SGN neurites over such a wide dose range, it is reasonable to expect ectopic neurite growth associated with the delivery of NT into the human cochlea irrespective of the delivery technique.

The present study did not address the long-term survival of SGN neurites following removal of their exogenous NT source. Given the retraction of neurites following loss of hair cells and supporting cells in the normal organ of Corti (i.e., their endogenous source of NT), and evidence of a loss of SGNs following the withdrawal of their exogenous NT source in deafened cochleae (Gillespie et al., 2003), there is an expectation of a significant retraction. However, there is evidence that chronic ES provides effective protection to SGNs following removal of NT (Shepherd et al., 2008), although that study did not directly evaluate long-term neurite survival.

Based on analysis of the neurite directionality data, neither NT nor ES treatment provided any significant guidance cues. Although SGN neurites have been shown to navigate toward localized NT sources *in vitro* (Wittig et al., 2005) and *in vivo* (Shibata et al., 2010; Wise et al., 2010), NT delivery via an osmotic pump, as used in the present study, presumably exhibits a minimal concentration gradient due to a rapid and widespread diffusion of the NT throughout the ST (Richardson et al., 2004; Plontke et al., 2007).

Although rare, we occasionally observed SGN neurites projecting across the OSL wall into the ST. Similar observations have been reported by others (Staecker et al., 1996; Glueckert et al., 2008; Leake et al., 2008, 2011; Wise et al., 2011). The OSL bone is thin and contains micropores (canaliculi perforantes; Lim and Kim, 1983; Shepherd and Colreavy, 2004), through which neurites may project. It is also possible that neurites enter the ST following a localized fracture of the OSL that can occur during the insertion of an electrode array. Many of the neurites projecting into the ST, as well as a small number that projected onto the basilar membrane, had a swelling at the tip reminiscent of a growth cone, although this could also be caused by an abnormality in the structural protein matrix of the neurites. It is unclear what prompts neurites to project into the ST, but they almost always appeared to do so through the OSL wall adjacent to the HP. Moreover, neurites within the ST are often associated with a fibrous tissue matrix (Leake et al., 2011; Wise et al., 2011), which could provide both physical and chemical support. There would be a number of functional advantages if the growth of neurites into the ST could be routinely promoted and directed toward the proximal electrode. Although there have been some attempts to develop stimulating electrodes that release neural guidance molecules—including NTs—to attract neurites, this work is in its infancy (Thompson et al., 2010).

Reduced thresholds associated with neurotrophin treatment

A significant reduction in the threshold of the electrically evoked ABR has been reported by a number of studies following chronic NT delivery to deaf cochleae (Shinohara et al., 2002; Shepherd et al., 2005; Landry et al., 2011; Leake et al., 2011). These results are consistent with the reduced ICC thresholds observed in the present study. Reduced thresholds may be caused by morphological changes in the SGN, such as increased diameter of neurites (Wise et al., 2005; Leake et al., 2011) and/or SGN soma (Shepherd et al., 2005; Agterberg et al., 2008; Glueckert et al., 2008; Landry et al., 2011; Leake et al., 2011), resulting in lower activation thresholds (McNeal, 1976). Changes in gene expression (e.g., voltage-gated ion channels) associated with NT treatment may also contribute to reduced electrical thresholds. For example, NT-3 and BDNF were shown to induce changes in the expression of several Ca^{2+} and voltage-gated potassium receptors in SGNs *in vitro* (Adamson et al., 2002).

Factors affecting spread of inferior colliculus activation

The spread of ICC activation was found to be associated with threshold, in agreement with a previous study in neonatally deafened and chronically stimulated cats (Moore et al., 2002). However, the threshold decreases caused by NT treatment in the present study did not result in corresponding decreases in STC width, suggesting that changes in threshold *per se* do not affect spatial selectivity of ES, and that some other factor was responsible. Given that this correlation was also found within the normal control group, which had similar SGN density across the cohort (Landry et al., 2011), it is probable that variation in the location of implant electrodes within the ST, which has a significant effect on activation threshold (Shepherd et al., 1993), was a contributing factor. The location of the electrode array relative to the neural elements can vary not only between animals, but also between different implant electrodes within animals due to the large and tapered nature of the ST in the guinea pig basal turn (Thorne et al., 1999). Positioning electrodes closer to the SGNs improves the spatial selectivity of intracochlear ES (Frijns et al., 2001).

In contrast to chronic NT treatment, we reported that the spread of neural activation within the ICC was significantly increased following chronic ES. Similar effects

have also been described by others (Snyder et al., 1990; Leake et al., 2000; Moore et al., 2002; Vollmer et al., 2007), although the mechanism(s) underlying this increased spread of activation is unclear. The increase in spread of ICC activation could potentially be a result of changes in one of a number of sites within the auditory pathway. Increased tissue growth within the cochlea following cochlear implantation and ES will result in altered current pathways that may produce broader excitation of SGNs, although we have seen no evidence that ES *per se* would evoke a greater tissue response than a chronically implanted US electrode array. Changes in excitatory/inhibitory synaptic mechanisms associated with deafness and/or cochlear implantation are known to occur within the various nuclei of the auditory brainstem (Ryugo et al., 2005, 2010; Tirko and Ryugo, 2012). For example, aged-related hearing loss is known to result in changes in pre- and postsynaptic γ-aminobutyric acid (GABA)ergic and glycinergic inhibitory neurotransmission within the central auditory pathway (Caspary et al., 2008). Although alterations in the balance of excitatory and inhibitory activity could result in increased spread of excitation within the ICC, evidence suggests that intracochlear ES reverses these deafness-related changes (Argence et al., 2008; Tirko and Ryugo, 2012), therefore minimizing the potential spread of activation. Importantly, there is no evidence of a reduction in spatial selectivity with cochlear implant use over time in a clinical setting; moreover, patient performance using these devices improves with device use (Blamey et al., 1996).

Clinical implications

The application of exogenous NTs to the deafened cochlea combined with chronic ES has the potential to improve the clinical outcome for implant patients compared with ES alone. Decreased thresholds to ES observed here and elsewhere (Shinohara et al., 2002; Shepherd et al., 2005; Landry et al., 2011; Leake et al., 2011) suggest that NT treatment can reduce power consumption of cochlear implants and allow the development of smaller intracochlear electrodes while still operating within safe charge density limits. The potentially negative impact of NT-enhanced neurite growth on the spatial selectivity of cochlear implants appears to be negligible, although it remains unclear whether more extensive ectopic growth of neurites would occur with longer treatment periods.

Clinically relevant techniques must be developed for safe long-term NT delivery to the cochlea. A major limitation associated with a pump/cannula-based system as used in the present study would be the risk of infection spreading from the pump/delivery system directly into the cochlea (Gillespie and Shepherd, 2005; Shepherd et al., 2005; Leake et al., 2011). Alternative strategies include the use of viral vectors (Stover et al., 2000; Kanzaki et al., 2002; Wise et al., 2010); encapsulated cell-based therapies using either naturally occurring (Wise et al., 2011) or genetically modified (Pettingill et al., 2011; Zanin et al., 2012) cells designed to express NTs; or biodegradable nonporous particles tuned for gradual NT release (Tan et al., 2012). The effects of long-term NT treatment using any of these delivery vehicles on both the cochlea and the central nervous system must be carefully addressed in safety studies prior to their clinical application.

Finally, these results may have application for other neural prostheses. There is considerable interest in combining knowledge from both functional ES and neural protection/regeneration studies in order to provide improved therapeutic outcomes via neural prostheses (Grill et al., 2001).

ACKNOWLEDGMENTS

Thanks to Mrs. H. Feng for implant manufacturing and contributions to implant design, Mr. R. Millard for engineering support and acoustic delivery software design, Mrs. A. Neil for surgical assistance, Dr. J. Xu for contributions to implant design and x-ray photography, and Prof. Peter Thorne for helpful advice on the delivery of the retrograde neural tracer.

CONFLICT OF INTEREST STATEMENT

To the best of our knowledge, there are no conflicts of interest.

ROLE OF AUTHORS

All authors had full access to the data and take responsibility for the integrity of the data and the accuracy of the data analysis. Study concept and design: all authors. Acquisition of data: TGL. Analysis and interpretation of data: all authors, primarily TGL. Drafting of the manuscript: TGL and RKS. Critical revision of the manuscript for important intellectual content: all authors. Statistical analysis: TGL. Obtained funding: all authors, primarily RKS, AKW, and JBF. Administrative, technical, and material support: all authors. Study supervision: RKS, AKW, and JBF.

LITERATURE CITED

Adamson CL, Reid MA, Davis RL. 2002. Opposite actions of brain-derived neurotrophic factor and neurotrophin-3 on firing features and ion channel composition of murine spiral ganglion neurons. J Neurosci 22:1385–1396.

Agterberg MJ, Versnel H, de Groot JC, Smoorenburg GF, Albers FW, Klis SF. 2008. Morphological changes in spiral ganglion cells after intracochlear application of brain-

derived neurotrophic factor in deafened guinea pigs. Hear Res 244:25–34.

Alam SA, Robinson BK, Huang J, Green SH. 2007. Prosurvival and proapoptotic intracellular signaling in rat spiral ganglion neurons in vivo after the loss of hair cells. J Comp Neurol 503:832–852.

Argence M, Vassias I, Kerhuel L, Vidal PP, de Waele C. 2008. Stimulation by cochlear implant in unilaterally deaf rats reverses the decrease of inhibitory transmission in the inferior colliculus. Eur J Neurosci 28:1589–1602.

Black RC, Clark GM, O'Leary SJ, Walters C. 1983. Intracochlear electrical stimulation of normal and deaf cats investigated using brainstem response audiometry. Acta Otolaryngol Suppl 399:5–17.

Blamey P, Arndt P, Bergeron F, Bredberg G, Brimacombe J, Facer G, Larky J, Lindstrom B, Nedzelski J, Peterson A, Shipp D, Staller S, Whitford L. 1996. Factors affecting auditory performance of postlinguistically deaf adults using cochlear implants. Audiol Neurootol 1:293–306.

Bohne BA, Harding GW. 1992. Neural regeneration in the noise-damaged chinchilla cochlea. Laryngoscope 102:693–703.

Caspary DM, Ling L, Turner JG, Hughes LF. 2008. Inhibitory neurotransmission, plasticity and aging in the mammalian central auditory system. J Exp Biol 211:1781–1791.

Dodson HC, Mohuiddin A. 2000. Response of spiral ganglion neurones to cochlear hair cell destruction in the guinea pig. J Neurocytol 29:525–537.

Ernfors P, Van De Water T, Loring J, Jaenisch R. 1995. Complementary roles of BDNF and NT-3 in vestibular and auditory development. Neuron 14:1153–1164.

Evans EF. 1972. The frequency response and other properties of single fibres in the guinea-pig cochlear nerve. J Physiol 226:263–287.

Fallon JB, Irvine DR, Shepherd RK. 2009. Cochlear implant use following neonatal deafness influences the cochleotopic organization of the primary auditory cortex in cats. J Comp Neurol 512:101–114.

Frijns JH, Briaire JJ, Grote JJ. 2001. The importance of human cochlear anatomy for the results of modiolus-hugging multichannel cochlear implants. Otol Neurotol 22:340–349.

Gillespie LN, Shepherd RK. 2005. Clinical application of neurotrophic factors: the potential for primary auditory neuron protection. Eur J Neurosci 22:2123–2133.

Gillespie LN, Clark GM, Bartlett PF, Marzella PL. 2003. BDNF-induced survival of auditory neurons in vivo: cessation of treatment leads to an accelerated loss of survival effects. J Neurosci Res 71:785–790.

Glueckert R, Bitsche M, Miller JM, Zhu Y, Prieskorn DM, Altschuler RA, Schrott-Fischer A. 2008. Deafferentation-associated changes in afferent and efferent processes in the guinea pig cochlea and afferent regeneration with chronic intrascalar brain-derived neurotrophic factor and acidic fibroblast growth factor. J Comp Neurol 507:1602–1621.

Grill WM, McDonald JW, Peckham PH, Heetderks W, Kocsis J, Weinrich M. 2001. At the interface: convergence of neural regeneration and neural prostheses for restoration of function. J Rehabil Res Dev 38:633–639.

Hardie NA, Shepherd RK. 1999. Sensorineural hearing loss during development: morphological and physiological response of the cochlea and auditory brainstem. Hear Res 128:147–165.

Henry BA, McKay CM, McDermott HJ, Clark GM. 2000. The relationship between speech perception and electrode discrimination in cochlear implantees. J Acoust Soc Am 108:1269–1280.

Kanzaki S, Stover T, Kawamoto K, Prieskorn DM, Altschuler RA, Miller JM, Raphael Y. 2002. Glial cell line-derived neurotrophic factor and chronic electrical stimulation prevent VIII cranial nerve degeneration following denervation. J Comp Neurol 454:350–360.

Landry TG, Wise AK, Fallon JB, Shepherd RK. 2011. Spiral ganglion neuron survival and function in the deafened cochlea following chronic neurotrophic treatment. Hear Res 282:303–313.

Leake PA, Hradek GT. 1988. Cochlear pathology of long term neomycin induced deafness in cats. Hear Res 33:11–33.

Leake PA, Snyder RL, Rebscher SJ, Moore CM, Vollmer M. 2000. Plasticity in central representations in the inferior colliculus induced by chronic single- vs. two-channel electrical stimulation by a cochlear implant after neonatal deafness. Hear Res 147:221–241.

Leake PA, Stakhovskaya O, Hradek GT, Hetherington AM. 2008. Factors influencing neurotrophic effects of electrical stimulation in the deafened developing auditory system. Hear Res 242:86–99.

Leake PA, Hradek GT, Hetherington AM, Stakhovskaya O. 2011. Brain-derived neurotrophic factor promotes cochlear spiral ganglion cell survival and function in deafened, developing cats. J Comp Neurol 519:1526–1545.

Liberman MC. 1982. Single-neuron labeling in the cat auditory nerve. Science 216:1239–1241.

Lim DJ, Kim HN. 1983. The canaliculae perforantes of Schuknecht. Adv Otorhinolaryngol 31:85–117.

Lim HH, Anderson DJ. 2007. Spatially distinct functional output regions within the central nucleus of the inferior colliculus: implications for an auditory midbrain implant. J Neurosci 27:8733–8743.

Martin RL, Webster WR, Serviere J. 1988. The frequency organization of the inferior colliculus of the guinea pig: a [14C]-2-deoxyglucose study. Hear Res 33:245–255.

McNeal DR. 1976. Analysis of a model for excitation of myelinated nerve. IEEE Trans Biomed Eng 23:329–337.

Miller JM, Chi DH, O'Keeffe LJ, Kruszka P, Raphael Y, Altschuler RA. 1997. Neurotrophins can enhance spiral ganglion cell survival after inner hair cell loss. Int J Dev Neurosci 15:631–643.

Miura M, Sando I, Hirsch BE, Orita Y. 2002. Analysis of spiral ganglion cell populations in children with normal and pathological ears. Ann Otol Rhinol Laryngol 111:1059–1065.

Moore CM, Vollmer M, Leake PA, Snyder RL, Rebscher SJ. 2002. The effects of chronic intracochlear electrical stimulation on inferior colliculus spatial representation in adult deafened cats. Hear Res 164:82–96.

Nadol JB Jr. 1997. Patterns of neural degeneration in the human cochlea and auditory nerve: implications for cochlear implantation. Otolaryngol Head Neck Surg 117:220–228.

Nadol JB Jr, Young YS, Glynn RJ. 1989. Survival of spiral ganglion cells in profound sensorineural hearing loss: implications for cochlear implantation. Ann Otol Rhinol Laryngol 98:411–416.

Pettingill LN, Wise AK, Geaney MS, Shepherd RK. 2011. Enhanced auditory neuron survival following cell-based BDNF treatment in the deaf guinea pig. PLoS One 6:e18733.

Plontke SK, Siedow N, Wegener R, Zenner HP, Salt AN. 2007. Cochlear pharmacokinetics with local inner ear drug delivery using a three-dimensional finite-element computer model. Audiol Neurootol 12:37–48.

Reiner A, Veenman CL, Medina L, Jiao Y, Del Mar N, Honig MG. 2000. Pathway tracing using biotinylated dextran amines. J Neurosci Methods 103:23–37.

Richardson RT, Wise A, O'Leary S, Hardman J, Casley D, Clark G. 2004. Tracing neurotrophin-3 diffusion and uptake in the guinea pig cochlea. Hear Res 198:25–35.

Richardson RT, O'Leary S, Wise A, Hardman J, Clark G. 2005. A single dose of neurotrophin-3 to the cochlea surrounds spiral ganglion neurons and provides trophic support. Hear Res 204:37–47.

Ryugo DK, Kretzmer EA, Niparko JK. 2005. Restoration of auditory nerve synapses in cats by cochlear implants. Science 310:1490–1492.

Ryugo DK, Baker CA, Montey KL, Chang LY, Coco A, Fallon JB, Shepherd RK. 2010. Synaptic plasticity after chemical deafening and electrical stimulation of the auditory nerve in cats. J Comp Neurol 518:1046–1063.

Shannon RV. 1983. Multichannel electrical stimulation of the auditory nerve in man. I. Basic psychophysics. Hear Res 11:157–189.

Shepherd RK, Colreavy MP. 2004. Surface microstructure of the perilymphatic space: implications for cochlear implants and cell- or drug-based therapies. Arch Otolaryngol Head Neck Surg 130:518–523.

Shepherd RK, Xu J. 2002. A multichannel scala tympani electrode array incorporating a drug delivery system for chronic intracochlear infusion. Hear Res 172:92–98.

Shepherd RK, Hatsushika S, Clark GM. 1993. Electrical stimulation of the auditory nerve: the effect of electrode position on neural excitation. Hear Res 66:108–120.

Shepherd RK, Coco A, Epp SB, Crook JM. 2005. Chronic depolarization enhances the trophic effects of brain-derived neurotrophic factor in rescuing auditory neurons following a sensorineural hearing loss. J Comp Neurol 486:145–158.

Shepherd RK, Coco A, Epp SB. 2008. Neurotrophins and electrical stimulation for protection and repair of spiral ganglion neurons following sensorineural hearing loss. Hear Res 242:100–109.

Shibata SB, Cortez SR, Beyer LA, Wiler JA, Di Polo A, Pfingst BE, Raphael Y. 2010. Transgenic BDNF induces nerve fiber regrowth into the auditory epithelium in deaf cochleae. Exp Neurol 223:464–472.

Shinohara T, Bredberg G, Ulfendahl M, Pyykko I, Olivius NP, Kaksonen R, Lindstrom B, Altschuler R, Miller JM. 2002. Neurotrophic factor intervention restores auditory function in deafened animals. Proc Natl Acad Sci U S A 99:1657–1660.

Snyder RL, Rebscher SJ, Cao K, Leake PA, Kelly K. 1990. Chronic intracochlear electrical stimulation in the neonatally deafened cat. I: Expansion of central representation. Hear Res 50:7–34.

Snyder RL, Bierer JA, Middlebrooks JC. 2004. Topographic spread of inferior colliculus activation in response to acoustic and intracochlear electric stimulation. J Assoc Res Otolaryngol 5:305–322.

Snyder RL, Middlebrooks JC, Bonham BH. 2008. Cochlear implant electrode configuration effects on activation threshold and tonotopic selectivity. Hear Res 235:23–38.

Spoendlin H. 1969. Innervation patterns in the organ of corti of the cat. Acta Otolaryngol 67:239–254.

Spoendlin H. 1984. Factors inducing retrograde degeneration of the cochlear nerve. Ann Otol Rhinol Laryngol Suppl 112:76–82.

Staecker H, Galinovic-Schwartz V, Liu W, Lefebvre P, Kopke R, Malgrange B, Moonen G, Van De Water TR. 1996. The role of the neurotrophins in maturation and maintenance of postnatal auditory innervation. Am J Otol 17:486–492.

Stankovic K, Rio C, Xia A, Sugawara M, Adams JC, Liberman MC, Corfas G. 2004. Survival of adult spiral ganglion neurons requires erbB receptor signaling in the inner ear. J Neurosci 24:8651–8661.

Stover T, Yagi M, Raphael Y. 2000. Transduction of the contralateral ear after adenovirus-mediated cochlear gene transfer. Gene Ther 7:377–383.

Sugawara M, Murtie JC, Stankovic K, Liberman MC, Corfas G. 2007. Dynamic patterns of neurotrophin 3 expression in the postnatal mouse inner ear. J Comp Neurol 501:30–37.

Tan J, Shepherd RK. 2006. Aminoglycoside-induced degeneration of adult spiral ganglion neurons involves differential modulation of tyrosine kinase B and p75 neurotrophin receptor signaling. Am J Pathol 169:528–543.

Tan J, Wang Y, Yip X, Glynn F, Shepherd RK, Caruso F. 2012. Nanoporous peptide particles for encapsulating and releasing neurotrophic factors in an animal model of neurodegeneration. Advanced materials 3:3362–3366.

Thompson BC, Richardson RT, Moulton SE, Evans AJ, O'Leary S, Clark GM, Wallace GG. 2010. Conducting polymers, dual neurotrophins and pulsed electrical stimulation—dramatic effects on neurite outgrowth. J Control Release 141:161–167.

Thorne M, Salt AN, DeMott JE, Henson MM, Henson OW Jr, Gewalt SL. 1999. Cochlear fluid space dimensions for six species derived from reconstructions of three-dimensional magnetic resonance images. Laryngoscope 109:1661–1668.

Tirko NN, Ryugo DK. 2012. Synaptic plasticity in the medial superior olive of hearing, deaf, and cochlear-implanted cats. J Comp Neurol 520:2202–2207.

Tong YC, Clark GM, Blamey PJ, Busby PA, Dowell RC. 1982. Psychophysical studies for two multiple-channel cochlear implant patients. J Acoust Soc Am 71:153–160.

Vollmer M, Beitel RE, Snyder RL, Leake PA. 2007. Spatial selectivity to intracochlear electrical stimulation in the inferior colliculus is degraded following long-term deafness in cats. J Neurophysiol 98:2588–2603.

Wise AK, Richardson R, Hardman J, Clark G, O'Leary S. 2005. Resprouting and survival of guinea pig cochlear neurons in response to the administration of the neurotrophins brain-derived neurotrophic factor and neurotrophin-3. J Comp Neurol 487:147–165.

Wise AK, Hume CR, Flynn BO, Jeelall YS, Suhr CL, Sgro BE, O'Leary SJ, Shepherd RK, Richardson RT. 2010. Effects of localized neurotrophin gene expression on spiral ganglion neuron resprouting in the deafened cochlea. Mol Ther 18:1111–1122.

Wise AK, Fallon JB, Neil AJ, Pettingill LN, Geaney MS, Skinner SJ, Shepherd RK. 2011. Combining cell-based therapies and neural prostheses to promote neural survival. Neurotherapeutics 8:774–787.

Wittig JH Jr, Ryan AF, Asbeck PM. 2005. A reusable microfluidic plate with alternate-choice architecture for assessing growth preference in tissue culture. J Neurosci Methods 144:79–89.

Ylikoski J, Pirvola U, Moshnyakov M, Palgi J, Arumae U, Saarma M. 1993. Expression patterns of neurotrophin and their receptor mRNAs in the rat inner ear. Hear Res 65:69–78.

Zanin MP, Pettingill LN, Harvey AR, Emerich DF, Thanos CG, Shepherd RK. 2012. The development of encapsulated cell technologies as therapies for neurological and sensory diseases. J Control Release 160:3–13.

Zilberstein Y, Liberman MC, Corfas G. 2012. Inner hair cells are not required for survival of spiral ganglion neurons in the adult cochlea. J Neurosci 32:405–410.

Zimmermann CE, Burgess BJ, Nadol JB Jr. 1995. Patterns of degeneration in the human cochlear nerve. Hear Res 90:192–201.